Quality Improvement Study

Medicine®

OPEN

Early-phase pelvic bone SPECT

Simulation and comparison of several acquisition protocols to reduce bladder artifact and improve image quality

Jacob Ayoubi, MSc[a,b], Sofiane Guendouzen, MSc[c], David Morland, MSc, MD, PhD[b,d,e,*]

Abstract

Tomoscintigraphic reconstruction in nuclear medicine assumes that the distribution of the tracer is unchanged in the volume of interest throughout the duration of the acquisition. This condition is however not met in early-phase bone scintigraphy and early-phase pelvic SPECT may display helical artifacts due to the filling of the bladder. Those artifacts may hamper proper interpretation of surrounding bone areas. The aim of this study was to construct a 4D digital pelvic phantom to simulate different acquisition protocols and optimize the acquisition.

A 4D digital pelvic phantom was generated with a dynamic component consisting in an expanding bladder with 2 ureters and a static part consisting in the 2 kidneys, bone structures, and soft tissues. Projection data were obtained using an attenuated Radon transform function. Four acquisitions protocols were tested: 32 projections of 16 seconds (32–16–1), 32 projections of 8 seconds (32–8–1), 2 consecutive SPECT of 32 projections of 4 seconds (32–4–2) and 2 consecutive SPECT of 16 projections of 8 seconds (16–8–2). The optimal protocol was then tested on one patient.

The amplitude of the artifacts was reduced with the 32–8–1, 32–4–2, and 16–8–2 protocols. The 16–8–2 protocol had the highest signal to noise ratio among those 3 protocols. The bladder artifact was visually markedly reduced on the patient acquisition with a 16–8–2 protocol.

Two successive early-phase bone SPECT, with a lower number of projection than the usual protocol reduce the impact of the helical artifacts around the bladder.

Abbreviations: HU = Hounsfield Unit, SNR = signal to noise ratio, SPECT = single photon emission computed tomography.

Keywords: bladder distortion artifact, dynamic phantom, early-phase bone scintigraphy

1. Introduction

Bone scintigraphy is an overly sensitive examination to assess bone turnover from the distribution of an intravenously injected radiotracer.[1] The images are acquired in several phases with schematically a first early acquisition showing the arrival of the tracer in the vascular network and soft tissues and a second late phase allowing the study of the bone. Single photon emission computed tomography (SPECT) significantly increased diagnostic sensitivity and specificity of bone scanning[1] but is most of the time reserved for the delayed phase.

The tomoscintigraphic reconstruction assumes that the distribution of the tracer is globally unchanged in the volume of interest throughout the duration of the acquisition, which can take several minutes. This condition is met for late images but not for early images during which, for example, a significant change in the quantity of tracer in the bladder can be observed due to its elimination. Bladder filling thus introduces reconstruction artifacts that may interfere with the nuclear physician's interpretation of the examination.

The aims of this study were twofold: the generation of a 4D digital pelvic phantom to simulate the distortion artifact due to the bladder filling; the simulation of several acquisitions protocol in order to optimize the acquisition.

2. Materials and methods

2.1. Digital phantom generation

The digital phantom gathered 2 distinct components: a dynamic component consisting in an expanding bladder with 2 ureters; a static part consisting in the 2 kidneys, bone structures, and soft tissues.

2.1.1. Static part of the phantom. The static part of the phantom derived from the segmentation of a late phase bone

Editor: Nagabhushan Seshadri.

All procedures performed in study involving human participants were in accordance with the ethical standards with the 1964 Helsinki Declaration and its later amendments.

The authors have no conflicts of interests to disclose.

The datasets generated during and/or analyzed during the current study are available from the corresponding author on reasonable request.

[a] Mines Saint-Etienne, Saint-Etienne, [b] Nuclear Medicine Department, [c] Medical Physics Department, Institut Godinot, [d] Biophysics Laboratory, UFR de Médecine, Reims, [e] CReSTIC, EA3804, Université de Reims Champagne-Ardenne, France.

[*] Correspondence: David Morland, Médecine Nucléaire, Institut Godinot, 1 rue du général Koenig CS80014, Reims Cedex 51726, France (e-mail: david.morland@reims.unicancer.fr).

How to cite this article: Ayoubi J, Guendouzen S, Morland D. Early-phase pelvic bone SPECT: simulation and comparison of several acquisition protocols to reduce bladder artifact and improve image quality. Medicine 2021;100:4 (e24473).

Received: 5 September 2020 / Received in final form: 25 December 2020 / Accepted: 4 January 2021

http://dx.doi.org/10.1097/MD.0000000000024473

SPECT acquired for clinical purpose. This SPECT was acquired 3 hours after the administration of 10 MBq/kg of 99mTc-HDP on a dual head Symbia T2 system (Siemens Medical Solutions, Forcheim, Germany) using the following parameters: step and shoot mode (32 projections of 10 seconds, 128×128 matrix). The acquisition was reconstructed using an OSEM 2D algorithm (2 iterations, 10 subsets) with a reconstructed voxel size of $4.8 \times 4.8 \times 4.8\,mm^3$.

Three tissues were segmented: soft tissues, kidneys and bones using thresholding and manual corrections. *InVesalius* software[2,3] was used to perform thresholding.

2.1.2. Bladder construction. The body of the bladder was modelized as a sphere and the 2 ureters were considered as cylinders. The measurements reported in the article of Lucacz et al[4] were used: maximal dimension of the sphere was 90 mm in diameter and the 2 ureters were 200 mm long with a diameter of 5 mm. Considering that we should be able to simulate a SPECT acquisition that last up to 15 minutes (900 seconds) with a minimal time per projection of 4 seconds, 225 (900/4) bladders of increasing size were created to simulate bladder filling. The lowest point of the bladder is fixed, whatever the bladder filling. *Autodesk Inventor 2020* software was used to build this digital bladder.

2.1.3. Structures combination and voxel value attribution. The static and dynamic parts mentioned above were combined. The final dimension of the matrix for each of the 225 phantoms was: $128 \times 128 \times 128$. The size of each voxel is $4.8 \times 4.8 \times 4.8$ mm^3.

The value of each voxel was assigned according to an adhoc estimation derived from a previously acquired early SPECT (summarized in Table 1). The 225 phantoms stacks were combined resulting in a 4D phantom of $128 \times 128 \times 128 \times 225$ voxels.

2.2. Projection data simulation

2.2.1. Attenuated Radon transform. A homemade Radon transform algorithm factoring photon attenuation was implemented in Python language (Equation 1). The linear attenuation coefficients μ_γ for 140 keV gamma photons were derived from the Hounsfield Units measured on the CT part of the SPECT used to construct the static component of the phantom (Equation 2).[5] The values are shown in Table 1.

$$R_a f(s,\theta) = \int_{-\infty}^{+\infty} f(s\theta + t\theta^{\perp})\, e^{-D_a(s\theta + t\theta^{\perp}, \theta^{\perp})}\, dt$$

Equation 1: The attenuated Radon transform equation. *f*: phantom image, *a*: attenuation map, θ: angle of projection, D_α: the attenuation distribution.

Table 1

values used for simulated tissues.

	SPECT (cps)	CT (HU)	μ_γ (cm^{-1})
Bladder	75	0	0.1500
Kidneys	150	25	0.1531
Bones	25	200	0.1750
Soft tissues	20	40	0.1550
Background	0	–1000	0

μ_γ: linear attenuation coefficient.
Cps = counts per second; HU = Hounsfield Unit.

$$\mu_\gamma = 0.15 + (1.52 + 0.03) * 10^{-4} * HU; for\, HU < 0$$

$$\mu_\gamma = 0.15 + (1.14 + 0.11) * 10^{-4} * HU; for\, HU > 0$$

Equation 2: Bilinear relationship between the linear attenuation coefficient and HU for 140 keV gamma photons.

2.2.2. Noise addition and delay function. Poisson noise was added to the projection data obtained with the attenuated Radon transform processing. A delay function was implemented to select the starting frame of the simulation. One minute is corresponding to 15 frames.

2.2.3. Simulations. Different projections data acquisitions were simulated as described in Table 2. The simulations are named after the following rule: "number of projections of a single SPECT – projection duration in seconds – number of time the SPECT is performed". In some cases (32–4–2 and 16–8–2), 2 temporally consecutive SPECT acquisitions were simulated, the resulting projection data corresponded to the sum of the 2 sets of projection data.

For all the simulations, a two-head gamma-camera was considered in "step and shoot" mode, the extent of rotation of each head was 180° (starting position for head 1: 0°, starting position for head 2: 180°).

Reference projections were also simulated for each acquisition protocol using a digital phantom derived from the 4D phantom without the bladder dynamic part.

2.3. Tomographic reconstruction

The tomographic reconstruction of the simulated projections was performed on a dedicated console (*Xeleris Workstation,* General Electrics, Milwaukee, USA) using *Volumetrix* software. Reconstructions parameters were as follow: OSEM 2D,[6] 2 iterations, 10 subsets, Butterworth filter: 0.48.

2.4. Quantification of the artefact

For each simulation, a signal to noise ratio (SNR) was calculated using the *SNR-plugin* developed by Sage et al[7] in *Fiji*.[8,9] The number of bone voxel whose value was significantly impaired by the bladder artifact was estimated. To be counted as an "impaired" bone voxel, 3 conditions had to be met:

- the bladder artifact can only influence the slices in which the bladder is present since the reconstruction is in 2D (OSEM 2D). Slices that never include the bladder, even at maximum filling, are therefore excluded.
- the voxel considered must correspond to a bone structure (the position of the bone structures is known by construction)
- the value of the voxel must vary with sufficient amplitude *A* between the simulation (bladder filling) and the reference (without bladder) as defined in Eq. (3).

$$A = \frac{|ri - reference|}{reference} - 1.96 * \sqrt{reference} > 0$$

Equation 1: Operation performed on the transaxials reconstructed images. It represents one of the conditions for a voxel to be counted as an impaired voxel. "ri" is the reconstruted image.

Table 2

Summary of the 4 types of simulated SPECT acquisition.

Name	32–16–1	32–8–1	32–4–2	16–8–2
Total number of projections (number of projections per head)	32 (16 × 2)	32 (16 × 2)	32 (16 × 2)	16 (8 × 2)
Projection duration (s)	16	8	4	8
Number of consecutive SPECT	1	1	2	2
Examination duration	512 s	256 s	256 s	256 s

"reference" is the reference image. The reconstructed image and the reference came from the same scenarios described in Table 2.

The mean amplitude of variation of the impaired bone voxels by averaging their respective *A* coefficients.

2.5. Patient acquisitions

Using the simulation results, the acquisition protocol was updated. An example of early bone SPECT acquisition using the acquisition protocol considered as optimal was acquired on an Intevo 6 system *(Siemens Medical Solutions, Forchheim, Germany)*, 4 minutes after the administration of 10 MBq/kg of 99mTc-HDP (step and shoot mode, 2 successive acquisitions of 16 projections of 8 seconds, 128 × 128 matrix) and reconstructed using the same algorithm as previously described. An early bone SPECT acquired with the previously used parameters (32 projections of 8 seconds) was used for comparison. The participants were informed of the possibility of using the information concerning them and had a right of opposition.

3. Results

3.1. Simulations

An axial slice at the same level for each scenario is showed in Figure 1. The helical artifact is visible, particularly for 32–16–1 and 32–8–1.

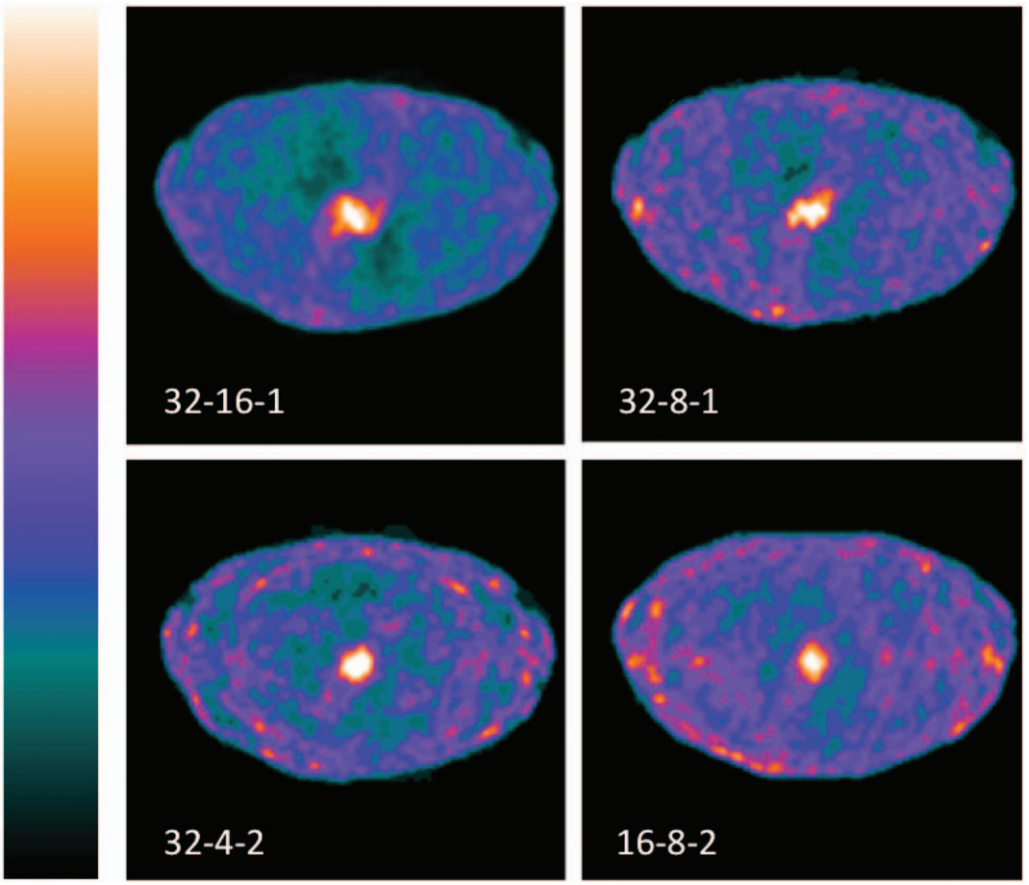

Figure 1. Resulting reconstructed images (axial slice 98) for each 4 simulated acquisition protocol. Top left-hand corner: simulation of a single SPECT acquisition of 32 projections of 16 seconds showing a helical distorsion of the bladder at the center of the image. Top right-hand corner: simulation of a single SPECT acquisition of 32 projections of 8 seconds, with a noticeable decrease of the signal to noise ratio and a less marked distorsion artefact. Simulation of 2 consecutive SPECT acquisitions of 32 projections of 4 seconds (bottom left-hand corner) and 2 consecutive SPECT acquisitions of 16 projections of 8 seconds (bottom right-hand corner) depicting a rounder bladder with less distorsion artefact.

Table 3

Resulting quality indicators for each reconstructed scenario.

Scenarios	32–16–1	32–8–1	32–4–2	16–8–2
Number of impaired bone voxels	90	45	52	89
Amplitude of variation	2.2	0.77	0.52	0.89
SNR	16.7	13.5	13.3	15.0

SNR, number of impaired bone voxels and amplitude of variation are reported in Table 3. Acquisition protocol 32–16–1 leads to the highest number of impaired voxels and the highest amplitude of variation and was not retained as optimal. Amplitude of variation was of the same order of magnitude in the remaining 3 scenarios, the acquisition protocol with the highest SNR was considered as optimal (scenario 16–8–2).

3.2. Patient acquisitions

We present in Figure 2 the early SPECT acquisitions of 2 patients, 1 using the (16–8–2) protocol, the other using the previously used acquisition protocol (32–8–1). The helical artefact is less visible with the (16–8–2) protocol.

4. Discussion

Bladder filling generates SPECT reconstruction artifacts requiring adaptation of the acquisition protocol. Our simulation faithfully reconstructed this helical artifact and allowed us to simulate different acquisitions.

The reduction of the acquisition time allows a reduction of this artifact, at the price of a reduction of the signal-to-noise ratio. In order to counter this effect, we tested the possibility of using 2 SPECT acquired sequentially rather than only one: the variation of the bladder size is lower within each SPECT and their addition restores the signal-to-noise ratio. Using too short projection times (4 seconds instead of 8 seconds) proved to be more harmful in our simulations than a decrease in the number of projections (16 vs 32) with SNRs of 13.3 for the (32–4–2) protocol vs 15 for the (16–8–2) protocol.

The number of bone voxels altered by the artifact is variable according to the scenarios but remains of the same order of magnitude and is very small compared to the total number of voxels present in the reconstructed volume. We focused on the amplitude of this variation and the signal-to-noise ratio to select the acquisition protocol that seemed optimal to us.

This protocol was successfully tested on a patient with a very noticeable reduction of the helix artifact and a good visualization of the vascular accumulation of the tracer in the other solid organs.

Some limitations of the simulation need to be addressed: the assignment of value to the voxels of the numerical phantom was made *adhoc*, helped by the non-optimized SPECT previously performed on patients in clinical routine. The lack of precise measurement probably explains the less marked character of the helix artifact on our simulations compared to patient acquisitions. We did not simulate multiple bladder filling rates or non-spherical shaped bladders.

5. Conclusion

The use of 2 successive SPECT with a reduced number of projections could decrease the bladder helical artifact often visible in early bone SPECT. Further studies will be needed to confirm these findings.

Author contributions

JA: simulation generation, data analysis, manuscript draft.
SG: data analysis, manuscript revision.
DM: study conception, data analysis, manuscript revision.
All authors read and approved the final manuscript.
Conceptualization: David Morland.
Data curation: Jacob Ayoubi.

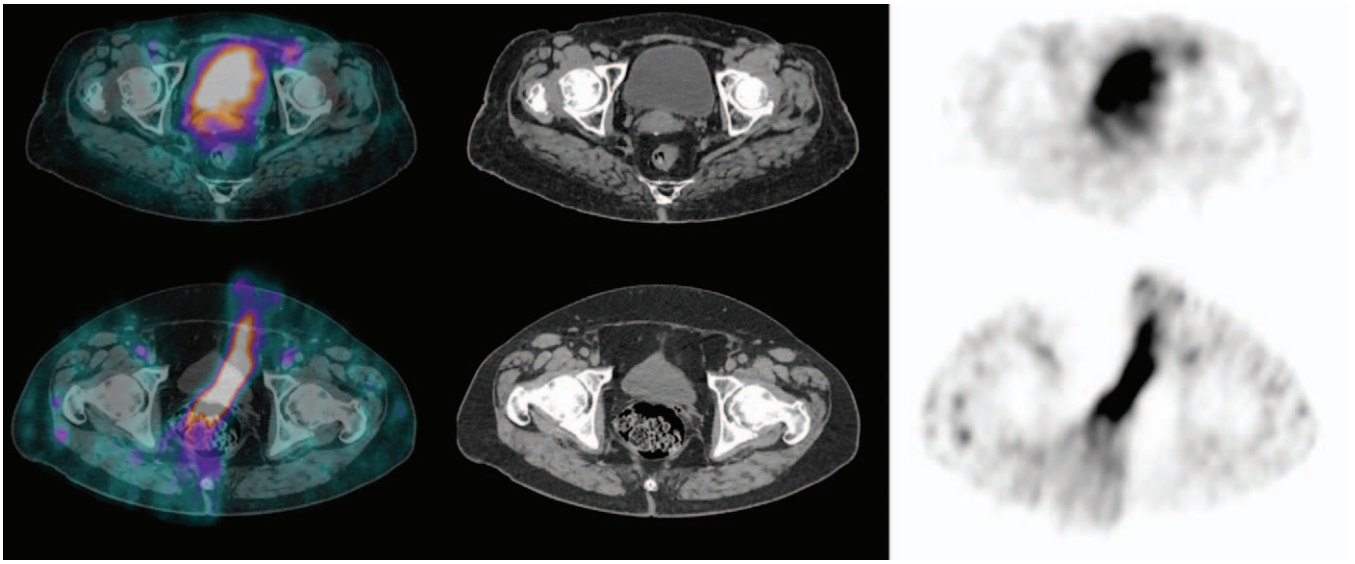

Figure 2. Early phase bone SPECT acquisitions and corresponding CT. Top line: acquisition using the (16–8–2) protocol. Activity is seen in the bladder, uterus, and left iliac vessels. No clear helical artefact is visible; bottom line: acquisition using the previously used acquisition protocol (32–8–1) with a marked distorsion of the bladder on the SPECT part of the acquisition.

Formal analysis: Sofiane Guendouzen, David Morland.
Methodology: David Morland.
Software: Jacob Ayoubi.
Supervision: David Morland.
Writing – original draft: Jacob Ayoubi.
Writing – review & editing: Sofiane Guendouzen, David Morland.

References

[1] Van den Wyngaert T, Strobel K, Kampen WU, et al. The EANM practice guidelines for bone scintigraphy. Eur J Nucl Med Mol Imaging 2016;43:1723–38.
[2] Moraes TF, Amorim PHJ, de Souza Azevedo F, Lopes da Silva JV. In Vesalius – An open-source imaging application. VIP Image 2011, Algarve, Portugal. Computational Vision and Medical Image Processing. London: Taylor & Francis Group 1; 2011:405–408.
[3] Amorim P, Franco de Moraes T, Pedrini H, et al. InVesalius: an interactive rendering framework for health care support. Int Sympos Visual Comput 2015;10.
[4] Lukacz ES, Sampselle C, Gray M, et al. A healthy bladder: a consensus statement. Int J Clin Pract 2011;65:1026–36.
[5] Brown S, Bailey DL, Willowson K, et al. Investigation of the relationship between linear attenuation coefficients and CT Hounsfield units using radionuclides for SPECT. Appl Radiat Isot 2008;66:1206–12.
[6] Alessio A, Kinahan P. PET image reconstruction. Nuclear Med 2006;1–22.
[7] Sage D, Unser M. Teaching image-processing programming in Java. IEEE Signal Process Magazine 2003;20:43–52.
[8] Rueden CT, Schindelin J, Hiner MC, et al. ImageJ2: ImageJ for the next generation of scientific image data. BMC Bioinformatics 2017;18:529.
[9] Schindelin J, Arganda-Carreras I, Frise E, et al. Fiji: an open-source platform for biological-image analysis. Nat Methods 2012;9:676–82.